Nuclear Materials and Energy 12 (2017) 334–340

Contents lists available at ScienceDirect

Nuclear Materials and Energy

journal homepage: www.elsevier.com/locate/nme

Studies of lithiumization and boronization of ATJ graphite PFCs in NSTX-U

F.J. Domínguez-Gutiérrez[a], F. Bedoya[b], P.S. Krstic[a,*], J.P. Allain[b], A.L. Neff[b], K. Luitjohan[c]

[a] Institute for Advanced Computational Science, Stony Brook University, Stony Brook, NY 11794-5250, USA
[b] Department of Nuclear, Plasma and Radiological Engineering, University of Illinois, Urbana, IL 61801, USA
[c] School of Material Engineering, Purdue University, West Lafayette, IN 47907, USA

ARTICLE INFO

Article history:
Received 16 July 2016
Revised 12 December 2016
Accepted 20 December 2016
Available online 27 December 2016

Keywords:
Plasma-surface interactions
Deuterium retention
NSTX
Boronization
Lithiumization
Carbon

ABSTRACT

This work examines the effect of boron and lithium conditioned ATJ graphite surface bombarded by low-energy deuterium atoms on the deuterium retention and chemical sputtering. We use atomistic simulations and compare them with experimental *in situ* studies with x-ray photoelectron spectroscopy (XPS), to understand the effects of deuterium irradiation on the chemistry in lithiated, boronized and oxidized amorphous carbon surfaces. Our results are validated qualitatively by comparison with experiments and with quantum classical molecular dynamic simulations. We explain the important role of oxygen in D retention for lithiated surfaces and the suppression of oxygen role by boron in boronized surfaces. The calculated increase of the oxygen role in deuterium uptake after D accumulation in B–C–O surface configuration is discussed. The sputtering yield per low energy D impact is significantly smaller in boronized than in lithiated surfaces.

1. Introduction

Conditioning of plasma facing components is an important enabling procedure for tokamak operation [1]. Conditioning with boron and lithium has led to improved performance in a variety of experimental fusion machines [2,3]. In the newly upgraded National Spherical Tokamak Experiment (NSTX-U), wall conditioning with deposition of boron has been used to provide fuel density control and impurity reduction [4,5]. Lithium will be used in the latter stage of the 2017 campaign with the same goal. NSTX-U is comprised of mostly carbon-based PFC (i.e. ATJ graphite tiles). Traditionally boron has been applied to the first wall of magnetic confinement machines via Plasma Enhanced Chemical Vapor Deposition (PE-CVD), using as mixture of a buffer gas e.g. He and a gas that contains B atoms e.g. diborane (B_2H_6) or trimethylborane ($B[CH_3]_3$) [6]. Boron coatings on Plasma Facing Components (PFCs) provide improved resistance to chemical sputtering and impurity retention thanks to a gettering effect associated with the formation of heavy oxides. However, erosion and passivation conjectured to be responsible for boron-associated improvements become only temporary and vanishing after tens to hundreds of plasma shots [3].

Li evaporation has also been used in different machines as a routine conditioning method [7,8]. In NSTX, Li evaporation decreased the H-mode access power threshold, increased the stored energy and allowed longer plasma discharges when compared with plasma discharges with no Li conditioning [8]. These improvements have been associated to the reduction of impurities and with the reduction of fuel recycling with the formation of Li–O–D complexes [9]. However as in the case of B, the erosion of the deposited Li layers added to its passivation with exposure to residual gas make the improvements to plasma transitory.

While the plasma performance is strongly influenced by the Plasma Facing Components (PFCs) the PFCs are modified with each exposure to the plasma. Critical to both an understanding and a practical operational strategy of tokamak PFCs with wall conditioning techniques is the role of surface chemistry over the entire plasma exposure. To establish this understanding both experiments and modeling have to be carefully planned and correlated and carried out as close as possible to the actual conditions in the tokamak to provide understanding of this synergistic relationship of the PFCs and plasma phenomena. In this paper we are using the atomistic theoretical approach, detailed in Section 2, to reveal hydrogen retention and sputtering in boronized and lithiated carbon

* Corresponding author.
E-mail address: predrag.krstic@stonybrook.edu (P.S. Krstic).

http://dx.doi.org/10.1016/j.nme.2016.12.028

materials under the bombardment of low energy deuterium atoms (5 eV), in various configurations and in combination with oxygen and accumulated deuterium. We combine our understanding obtained from atomistic simulations to a combination of state-of-the art in-situ experimental measurements that includes the Materials Analysis Particle Probe (MAPP) [10] diagnostic capable of *in situ ex tempore* (e.g. in between plasma shots) operated in NSTX-U divertor region. This experimental approach enables for the first time insight in the evolution of surface chemistry at the time scale of surface modification exposed to tokamak plasmas. This methodology, complementary to controlled experiments and modeling, allows "on line" study of the chemistry of the surfaces with no exposure to external atmosphere and with time resolution of adjacent plasma shots, a huge improvement compared with post-mortem characterization i.e. end of one experimental campaign (thousands of plasma shots). The theoretical and experimental approaches are described in the Methods Section 2. Our results are presented in Section 3. Section 4 contains our conclusions.

2. Methods and materials

2.1. Theoretical

Our atomistic simulations are based on Classical Molecular Dynamics (CMD), using Reactive Force Field (ReaxFF) Bond Order (BO) potential [11] in the Large Scale Atomic/Molecular Massively Parallel Simulator (LAMMPS) [12]. We verify the CMD calculations by Quantum-Classical Molecular Dynamics (QCMD), using approximate Self Consistent Charge Tight Binding Density Functional Theory (SCC-DFTB) [13,14] to compute electronic motions in the adiabatic limit of nuclear motion. We choose ReaxFF for its capabilities to model dynamics of breaking and forming of chemical bonds [15], as well as to calculate the dynamic changes of charges of the atoms in the system using Electronegativity Equalization Method [16,17]. The latter is particularly important in the presence of mutually polarizable materials such as lithium, boron, and oxygen.

We use computational cell of about 400 atoms for various amorphous mixtures of Li, B, C, and O. Boronized, lithiated and oxidized systems are created by random substitution of carbon atoms to the desired atomic concentrations, estimated by the experiment to be atomic composition of (20, 60, 20) % for B,C,O respectively. The same composition was assumed for the Li,C,O composition. The mixtures are then annealed and finally thermalized to 300 K and energy optimized with periodic boundary conditions in the x-y directions (Fig. 1), following the procedure of Krstic et al. [18,19]. This procedure allows the formation of complexes with the chemical properties studied in this paper. Additional reformation of the chemical complexes evolves upon bombardment by D atoms, as explained below. It is interesting to note that upon thermalization and energy optimization the B–C–O surface of the composition (20, 60, 20) % has size 17 Å in the z directions, whereas the lithiated Li–C–O cell with the same configuration expands in z-direction up to 24 Å. To take into account typical experimental conditions of the accumulated deuterium, the cells were prepared by cumulative bombardment by 5 eV D atoms, reaching various atomic concentrations of D. The penetration of D at 5 eV was distributed in depth up to 8 Å, and therefore the atomic concentrations $\frac{n_D}{n_D+n_C+n_B+n_O} \times 100\%$ were defined for the part of the computation cell from the top surface to 8 Å depth. The highest accumulated concentration of D reached was 28%, and this corresponds to the D saturation at the considered impact energy. The sufficient time (50 ps) was taken for the evolution cascade, and the cell is thermalized and relaxed after each impact. After the computational cell is prepared, either with no D or with some % of accumulated D, it is bombarded by 3100 independent 5 eV D trajectories, orthogonal to the surface. Each of these trajectories were

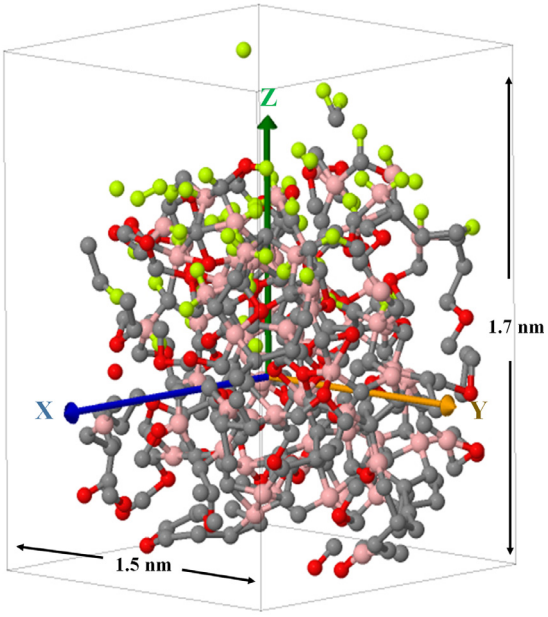

Fig. 1. Computational cell is mixture of Li or B (pink) with C (gray) and oxygen (red), with accumulated D (green) atoms in the top surface layers upon bombardment with D. The z-axis is shown by the arrow. (For interpretation of the references to color in this figure legend, the reader is referred to the web version of this article.)

hitting the same prepared surface but at random locations in order to obtain adequate statistics. Each result reported here is therefore obtained as average from 3100 D trajectories. The retention chemistry of D evolves at the end of the collision cascade when the impact particle is thermalized allowing comparison with the experimental results at higher impact energies [19]. We carry out the analysis of the resulting chemistry after the final rest location of each D impact, by performing the nearest-neighbor (NN) calculation for each atom in the surface, defining the coordination number of each atom and the most-probable bonds [19]. Example of such analysis is shown in Fig. 2, performed by both CMD and by quantum-mechanical QCMD**.** The results in Fig. 2 for BCO mixture are dramatically different than those obtained for LiCO mixture in [19]. Namely, while in case of LiCO main role in bonding of D is played by oxygen, here that role is dominated by boron. Boron is more reactive than oxygen because of the so-called octet rule, i.e. a coordination number of four is preferred for B atoms, and in our simulations we sometimes even find coordination numbers of five and six, enabling larger number of D to bond to a B atom than to oxygen (with typical coordination number 2). Also electron withdrawing ligands on B such as O further increase D uptake on B. The role of B in the retention of D does not change with increasing D accumulation.

It is interesting to note that QCMD calculation is by several orders in magnitude slower and much more numerically involved than the CMD. Thus, the SCC-DFTB calculations at Fig. 2 was performed at the Titan Cray XK-7 machine using about 50,000 cores and 3000 GPU units (2025 trajectories), while the LAMMPS calculation was performed at the IACS LIred institutional cluster. In spite of a big difference in computational load, both calculations give the qualitatively similar results.

2.2. Experimental

As mentioned above, boronization was used in the early stage of the 2015 experimental run in NSTX-U. Boron is applied in NSTX-U using deuterated-trimethylborane via a 95% He + 5% D-TMB DC

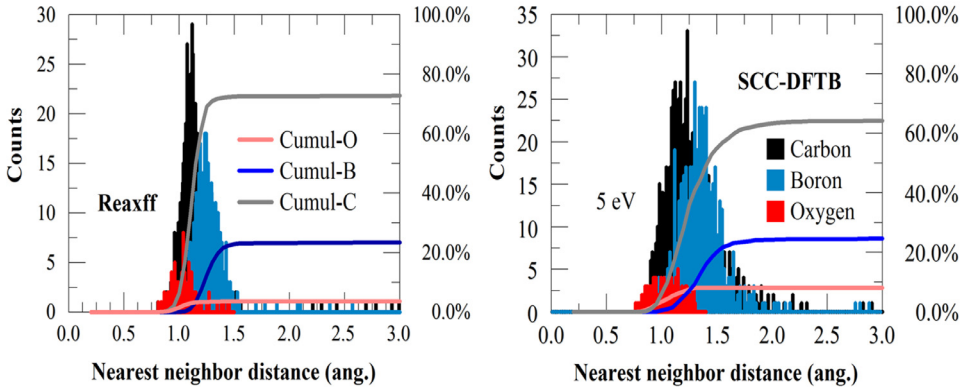

Fig. 2. Nearest neighbor analysis for retained D trajectories in a sample of 20% of boron and oxygen in the carbon, prepared by ReaxFF in LAMMPS (left) and by QCMD with SCC-DFTB (right). Both approaches show the effect of the oxygen suppression in the retention chemistry, though with slightly different cumulative numbers and the distribution widths.

glow that lasted between four and six hours, this usually resulted in deposition of ~7 nm of B_4C on the lower divertor [4,5]. The frequency of the boronizations varied from every two weeks to daily, depending on the experimental plan and the plasma behavior. The Materials Analysis Particle Probe (MAPP) [10] was used for *in situ ex-tempore* characterization of an ATJ sample, exposed to boronizations and plasma discharges. X-ray Photoelectron Spectroscopy (XPS) was taken before boron deposition, shortly after boronizations and following each day of plasma operations (around 20–25 D^+ plasma shots). The samples are inserted in the lower divertor of NSTX-U and exposed to the boronization glow. After that these are retracted to the analysis chamber for XPS characterization. Following these measurements the samples are re-inserted to the tokamak's vacuum vessel. There these are exposed to daily plasma discharges and retracted at the end of every run day for data collection. The C1s, O1s and B1s photoelectric peaks were measured every night. The data is analyzed using peak deconvolution to check the evolution of the chemical bonding [20] with various plasma exposure conditions.

Additional experiments were carried out in an attempt to explain more fully the role oxygen plays in D retention in lithiated graphite as has been observed previous [18,19]. These tests were performed in the PRIHSM (Particle Radiation Interaction with Hard and Soft Matter) facility at Purdue University. Square ATJ carbon samples (1 cm^2) were irradiated with D at 500 eV/amu up to a fluence of 1×10^{18} cm^{-2} to remove all surface oxygen. This is shown in the XPS results in Fig. 3. In particular, the O1s response is shown in Fig. 3(c) where the initial irradiation with D_2 ions *in-situ* is shown to eliminate all oxygen (see: second curve from bottom). After the initial irradiation, a 2 μm coating of Li was deposited from a thermal evaporation source, noting that the deposition leads to co-deposition of oxygen. Following lithium deposition, the sample was again irradiated with D in incremental steps of about 2×10^{17} cm^{-2} after reaching an initial fluence of 1×10^{17} cm^{-2}. Irradiation was completed at 9×10^{17} cm^{-2}. Note that the relative peak of Li–O–D to O–Li in the O1s increases with D_2 fluence and this is further corroborated by high-flux tests. High flux ($\sim 1 \times 10^{19}$ $cm^{-2}s^{-1}$) tests were also carried out at the Dutch Institute for Fundamental Energy Research (DIFFER) on similar ATJ samples. The irradiation was similar with an initial D plasma exposure to remove oxygen from the surface, following the recipe form *in situ* tests, and then full D plasma exposure after Li was deposited. Deposition of a 2-μm Li layer also resulted in a reaction between D implanted atoms, oxygen and lithium prior to the post-Li deposition D_2 irradiations. Details of the high flux tests are provided in previous work [21]. The fluence reached for these samples was 3×10^{20} cm^{-2}. These samples were analyzed with XPS after irradiation and required sputter cleaning to examine the chemistry below the passivation layer that formed on the Li surface following exposure when the sample was exposed to atmosphere for transport.

3. Results

In Fig. 3, we present XPS results from the controlled *in situ* ion beam experiments performed in PRIHSM (Fig. 3(a)–(c)) included with the XPS results, Fig. 3 also shows the simulation results for the bonding percentage of C (Fig. 3(d)), Li (Fig. 3(e)), and O (Fig. 3(f)), both to themselves and to other species in the simulation matrix. In particular, the simulations include the case for accumulated D in the complex Li–C–O–D system, which gives critical insight on the role of O in the surface response when exposed to D plasma. The experimental study (a–c) observed the formation of Li–C–D and Li–O–D functionalities after exposure to D ions at low flux, ($\sim 4 \times 10^{14}$ $cm^{-2}s^{-1}$). The post mortem results (not shown here) from tests in the high-flux plasma facility ($\sim 1 \times 10^{19}$ $cm^{-2}s^{-1}$) at the Dutch Institute for Fusion Energy Research (DIFFER), described in Section 2.2, did not show deviation of these functionalities when high plasma fluxes of D ions is applied. Although XPS cannot directly measure the presence of D in the matrix, D interactions with C, Li and O atoms are detected through the Li–C–D and Li–O–D peaks in photoelectron spectra [22]. The Li–C–D complex in Fig. 3(a) assigned at 292.1 eV is observed at fluence larger than about 10^{17} cm^{-2}, providing an evidence for the D fluence threshold for the complex formation. The C–O peak increases with D fluence, even dominating the Li-C-D peak, while graphitic (C–C) decreases with D-fluence. In Fig. 3(b), Li–O–D peak exists and increases with the D fluence. Finaly, in the O1s spectra in Fig. 3(c), the O–Li peak appearing upon lithiumization of the carbon surface, shows decrease with the D fluence increase, while Li–O–D increases, confirming the role that O plays in retention of D in carbon [17]. The simulations, in 3d–f, elucidate these interactions demonstrating that it is the accumulation of D that results in the increased number of bonds of D and O atoms in the complex Li–C–O system. Percentage of oxygen as well as Li in all configurations in Fig. 3(d)–(f) is kept at about 20%. Thus, C–C bonding decreases significantly in LiCO and LiCOD configurations in comparison to LiC, while C–O bonding decreases in LiCO and LiCOD configurations in comparison to CO at Fig. 3(d). Also, Li–O bonding slightly increases in LiCOD configuration in comparison to LiCO, while Li–C decreases in LiCO and LiCOD configurations in comparison to LiC in Fig. 3(e). Finally, O–Li and O–C bonding slightly decreases in LiCOD configuration in comparison to LiCO in Fig. 3(f). We note that most of C atoms are bonded to C in 3d, most of Li

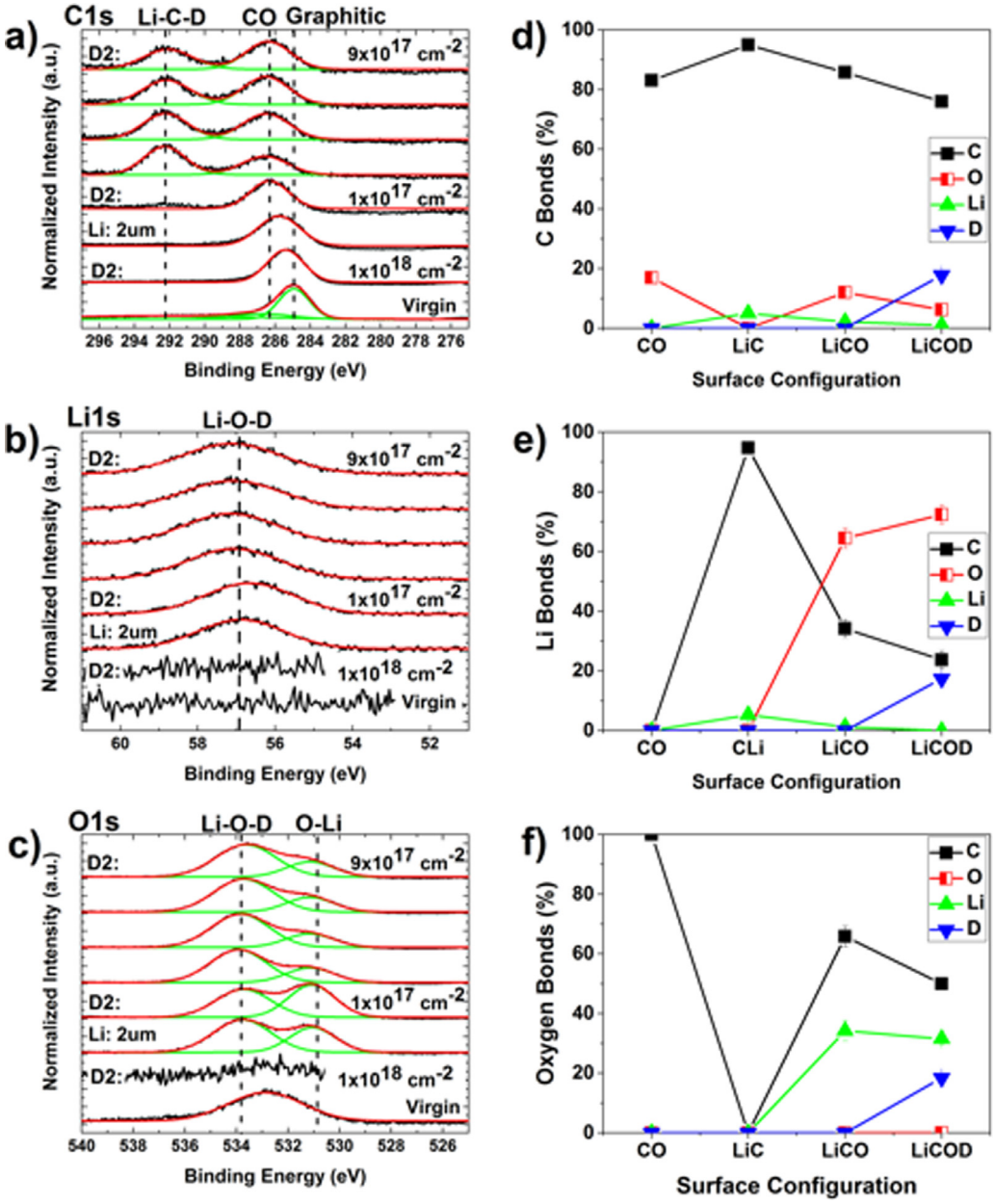

Fig. 3. (a)–(c) *In situ* XPS results from controlled D irradiation for the C 1 s, Li 1 s, and O 1 s regions. The plots on the right, (g)–(i), are *post mortem* XPS of samples exposed at DIFFER of the same regions. The simulation results, (d)–(f), are oxygen, carbon and lithium chemistry for various configurations, CO, LiC, LiCO and LiCO after preparing the sample by bombardment by D, until reaching accumulation of 28%. Statistics was taken for 3000 random 5 eV D trajectories.

atoms are bonded to O in 3e, and most of O atoms are bonded to C, together with significant number of bonds to Li in 3f. The absence of the expected three peaks (C–O, Li–O, Li–O–D) in Fig. 3(c), where likely the C–O and Li–O interactions are effectively at very close binding energies and not resolved in this data. The simulations aid in explaining this in Fig. 3(b) with the Li1s spectra and Fig. 3(e) where the accumulation of D results in Li atoms bound preferentially to D and O and less to C. This is also corroborated by *in situ* data in Fig. 3(a) where the Li–C–D peak is not very strong after deposition of Li on a ATJ graphite substrate with implanted D atoms. The *in situ* ion beam results shown in Fig. 3(c) indicate the complete removal of oxygen from the surface observed in the O1s spectra after irradiating with D before depositing Li. When the Li is deposited, oxygen is observed in the XPS indicating the introduction of oxygen with Li deposition, an effect known to occur during lithiumization steps in NSTX-U. Upon continued irradiation with D the Li–O–D complex forms at $1 \times 10^{17}\,\mathrm{cm}^{-2}$ and persists as irradiation continues. This effect is again supported by observation from the atomistic simulations. There is a clear corresponding increase of interactions of D with O with accumulated D in the system.

Fig. 4(a) shows the O1s photoelectric peak region scan taken from an ATJ sample in NSTX-U. The figure displays three different states of the sample. Initially a base line was collected on the untreated sample, a single peak, assigned to C–O is observed at ~532 eV. Following boronization, the sample develops two other functionalities, illustrated by one peak assigned to B–O interactions around 531 eV and a second peak at ~533 eV associated with O–B–D interactions. The appearance of these peaks following the boron deposition is justified by the reaction of the energetic particles in the He glow discharge (used during boronization) with background gases *e.g.* water vapor and deuterium contained in d-TMB.

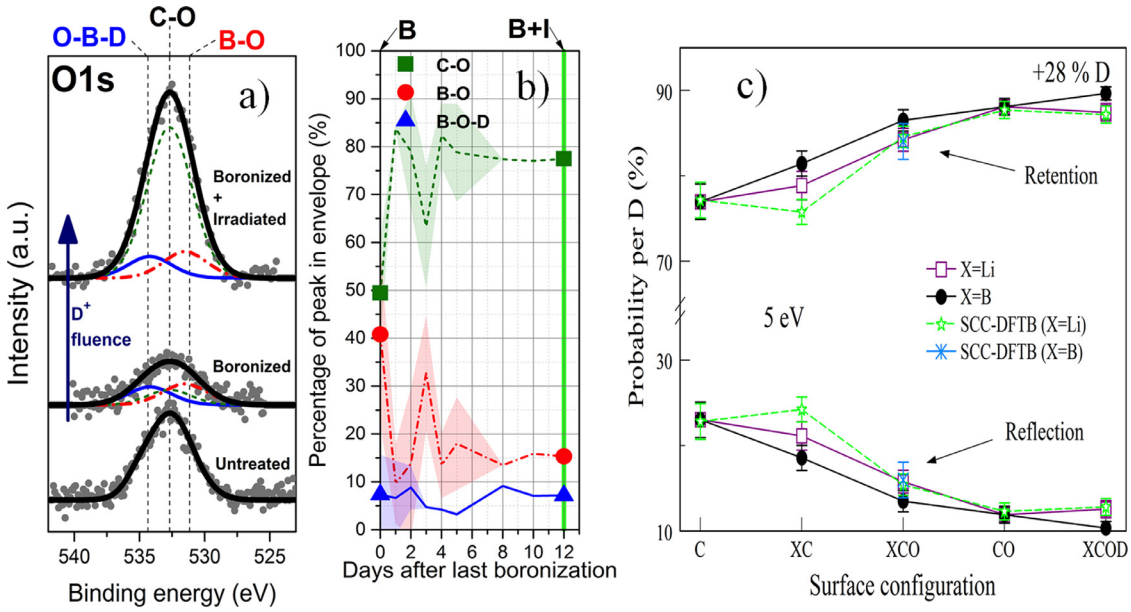

Fig. 4. (a) O1s XPS region showing D retention (area of O-B-D peak [19]) of D in NSTX-U, (b) Percentage of each component in the total XPS envelope (on Fig. 4(a)) as a function of time after a boronization, the shown data points are the average over three boronizations and the shaded error bars show the standard deviation of the data set (only one data set had data after day 8 thus the zero standard deviation); (c) Computer simulations results of D uptake and reflection probabilities for D impact at various surface configurations with lithium and boron. XCOD surface has about 30% of D.

In Fig. 4(b), we present computer simulations for D uptake and reflection probabilities at various boronized and lithiated surface configurations, using both CMD and, in case of Li, also QCMD. The C-only surface shows the lowest deuterium retention with about 77% of D retained. Boron- carbon (BC) mixture (20, 80) % increases the D retention more efficiently than lithium in carbon (LiC (20, 80) % mixture), with a difference in the total retention probability about 3%. However, when oxygen is present in both configurations this difference decreases to 2%. For the case of D accumulation, the results for the same percentage of D accumulated in the LiCO and BCO surface configurations of about 30% in the upper half of the simulation cell, show dominance of the B–C–O retention, mainly because the increased role of boron (valence 3) in the D bonding in comparison to Li. We compare our results also with the previous QCMD calculations of Krstic et al. [19], showing difference in retention of about 3% only for case of LiC. In spite of the quite different chemistry of B and Li to deuterium, the retention probabilities are quite similar.

Fig. 4(a) allows to see retention of deuterium by the boronized graphite samples after plasma irradiation. Following the exposure to D^+ ions the O–B–D peaks seems to increase its area this implying an increased retention of D by the oxygen in the samples. This retention with high D contents can be compared with the points at the higher end (right side) of Fig. 4(a) where the retention of D seems to increase for the BCOD configuration with 28% D concentration. This observation is further confirmed by Fig. 4(b), wherethe contribution to the total XPS peak from each chemical environment is shown as a function of time following a boronization. Although the increase in the O–B–D peak is not dramatic in Fig. 4(b), the formation of that bonding and its incremental dependence on fluence is almost clear. It is worth mentioning that the XPS data also shows sputtering and oxidation of the B coatings due to the interaction with the plasma, this is most likely the reason why we observe only small increase in the O–B–D formation.

In Fig. 5 we show calculated total and carbon sputtering yield per incident D for various surface configurations, total ejection yield per D is considered as a summation of all atoms and molecules ejected from the surface mixture. We compare the results for boronized and lithiated surfaces. The ejection yield of carbon is significantly smaller for BC than LiC configurations (stronger interaction of B–C than Li–C), especially in presence of oxygen, which suppresses sputtering in both cases. We also compare our results for lithiated surfaces with the QCMD results [17], which show the same trend. It is interesting to stress that in each case LiC mixture (without oxygen) has the largest erosion yield. We also stress that, unlike retention rate, the sputtering yield is a strong function of impact energy. Here we show the erosion results close to the lower energy threshold for the chemical erosion. Sputtering of various Li and B mixtures at higher energies will be subject of future publications.

In Fig. 6 we show the percentage of sputtering yield per incident D for different ejected molecules as function of the lithiated surface configurations, calculated by CMD. The majority of sputtered material is in form of molecules, which are diatomic at these low, 5 eV D, energies. We notice that CD molecules are majority for all configurations, the highest being for LiC surface and the lowest at CO surface. Whenever oxygen is present there is a significant reduction of CD ejection, as is a case in LiCO surface. The highest yield of LiD molecules is for LiC target. OD eject rate is the same for both LiCO and deuterated LiCO surfaces.

The contributions to the ejection yield per incident D in form of various diatomic molecules (and atomic oxygen) for boronized surface configurations, calculated by CMD, are shown in Fig. 7 where the starting point is the BC surface with an atomic distribution of 20% of B and 80% of C, then we substitute different percentage of C by oxygen until to reach an atomic distribution of 20% of B and O, and 60% of C which is called the BCO surface mixture. The next step is to analyze the chemical sputtering from the deuterated BCO surface by considering different amounts of deuterium in the BCO surface obtained; the saturated system is at 28% of D accumulated. Appearance of water ejection for case of the accumulated D is remarkable. Presence of oxygen increase the oxygen ejection, but significantly decrease the CD ejection.

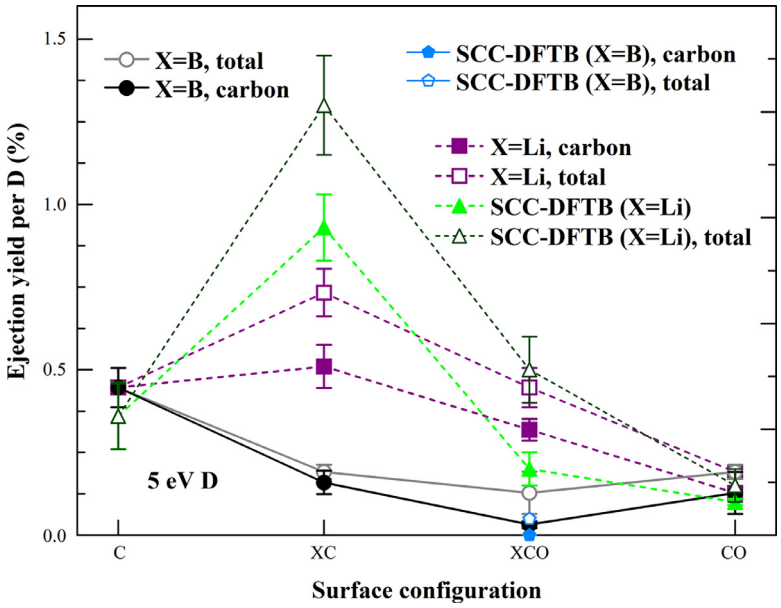

Fig. 5. Total and C ejection yield per D for various surfaces configurations comparing the carbon erosion for boronized and lithiated surfaces, and comparing different methods of calculation (CMD with ReaxFF and QCMD with SCC-DFTB [17]).

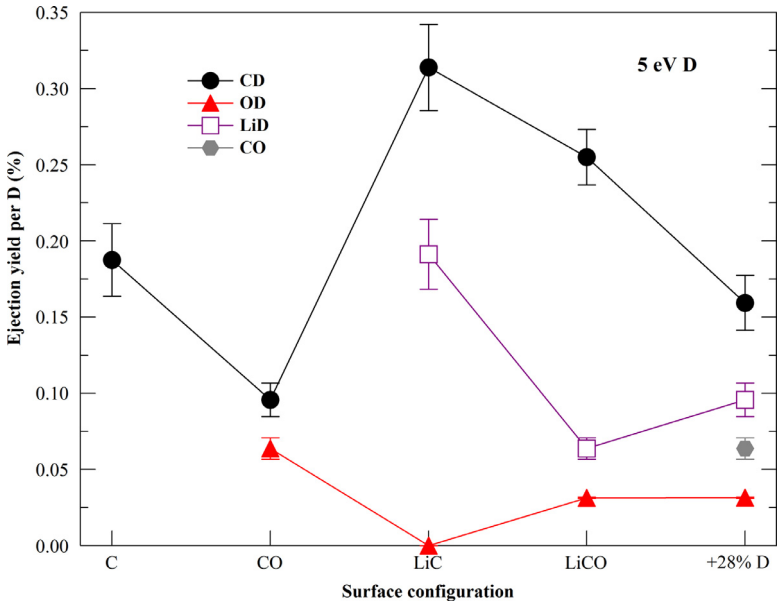

Fig. 6. CMD results for the ejection yield per D (%) for CD (black circles), OD (red triangle), LiD (black squares), and CO (gray pentagon) molecules as function of the surface configurations. (For interpretation of the references to color in this figure legend, the reader is referred to the web version of this article.)

4. Summary and conclusions

We have performed atomistic simulations, combining CMD and QCMD, to obtain retention of deuterium and sputtering of lithiated, boronized and oxidated amorphous carbon surfaces exposed to the 5 eV deuterium impacts. We have also done the laboratory XPS experiments by exposing lithiated ATJ carbon to the beam deuterium of 500 eV/amu energy, a high flux D plasma at DIFFER, and *in-situ ex-tempore* XPS experiments inside the NSTX-U vessel of exposing boronized carbon to the deuterium plasma. The experimental and theoretical data show a reasonable qualitative agreements for both lithiated and boronized surfaces. Using the computational simulations we compare the deuterium retention probabilities and chemical sputtering yields of lithiated and boronized surfaces in various configurations. Though both boronized and lithiated surfaces show similar trends in retention of deuterium when composition of the material is varied, the former surfaces show somewhat higher degree of retention, less dependent on the oxygen content than in case of lithiated surfaces. On the other hand, chemical sputtering of the surface material at considered low impact energy is significantly lower with boronized surfaces than with the lithiated ones, though both results are improved with a content of oxygen in the material. While in case of the lithiated surfaces CD and LiD are dominating the sputtered material, potentially emitted into the plasma, CD and D_2O are dominating the emitted molecules from boronized surfaces, which becomes exclusively D_2O with increase of the D accumulation. Chemical sputtering, unlike the retention probability, is strongly dependent on the impact energy. This energy dependence for the material matrices considered here is numerically intensive and will be a subject of our forthcoming work.

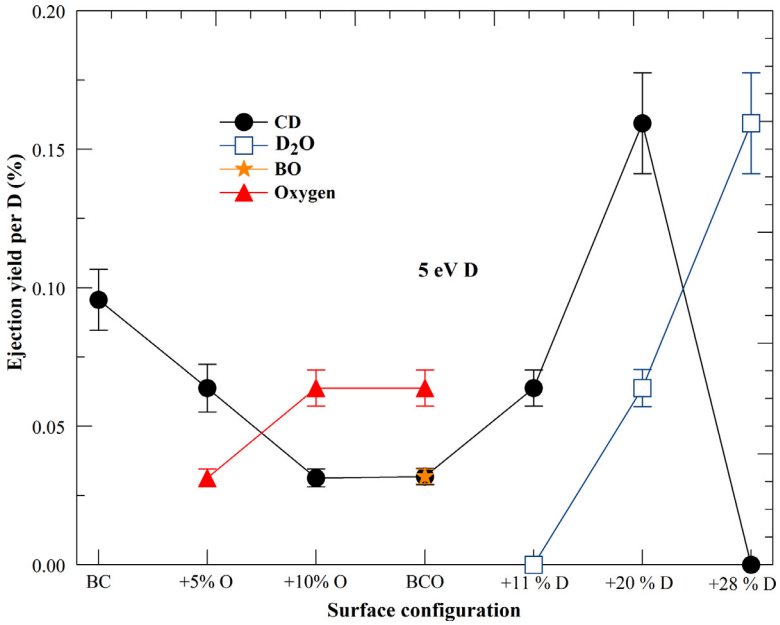

Fig. 7. CMD results for the ejection yield per D (%) for CD (black circles), Oxygen atoms (red triangle), BO (orange star), and D_2O (empty square points) molecules as function of the boronized surface configurations at difference oxygen concentrations and percentages of deuterium accumulated. (For interpretation of the references to color in this figure legend, the reader is referred to the web version of this article.)

Funding sources

This work was supported by National council for Science and Technology of Mexico (CONACyT) through the postdoctoral fellowship CVU 267898 (FJDG), by COLCIENCIAS through the Francisco Jose de Caldas Fellowship Program and the U.S. Department of Energy Office of Science, Office of Basic Energy Sciences Fusion Energy Sciences Program under Grant No. DE-SC0010717 (JPA and FB), by DOE FES Grant No. DE-SC0013752 through RF of SUNY (PSK).

Acknowledgements

Simulations were obtained using the LI-red cluster at the IACS-SBU, by the NCCS supercomputing facility in ORNL, and by the XSEDE computing facilities. We are grateful to professor Adri van Duin of Penn State University for inspiring discussions on the REAXFF.

References

[1] J. Winter, Plasma Phys. Control. Fusion 38 (1996) 1503.
[2] R. Maingi, S.M. Kaye, C.H. Skinner, et al., Phys. Rev. Lett. 107 (2011) 145004.
[3] C. Hollenstein, B.P. Duval, T.D. de Wit, et al., J. Nucl. Mater. 176 (1990) 343.
[4] F. Bedoya, J.P. Allain, R. Kaita, et al., in: Proceedings on International Conference in Plasma Surface Interactions in Controlled Fusion Devices 22nd PSI, Rome, Italy, 2016.
[5] C.H. Skinner, J.P. Allain, F. Bedoya, et al., in: Proceedings on International Conference in Plasma Surface Interactions in Controlled Fusion Devices 22nd PSI, Rome, Italy, 2016.
[6] O.I. Buzhinskij, Y.M. Semenets, Fusion Sci. Technol. 32 (1997) 1–13.
[7] M. Lucia, R. Kaita, R. Majeski, et al., J. Nucl. Mater. 463 (2015) 907.
[8] H. Kugel, D. Mansfield, R. Maingi, et al., J. Nucl. Mater. 390 (2009) 1000.
[9] C.N. Taylor, Doctoral, Purdue University, West Lafayette, IN, USA, 2012.
[10] M. Lucia, R. Kaita, R. Majeski, et al., Rev. Sci. Instrum. 85 (2014) 835 11D.
[11] A.C.T. van Duin, S. Dasgupta, F. Lorant, et al., J. Phys. Chem. A 105 (2001) 9396.
[12] S. Plimpton, Fast parallel algorithms for short-range molecular dynamics, J Comp Phys. 117 (1995) 1–19.
[13] M. Elstner, D. Porezag, G. Jungnickel, et al., Phys. Rev. B 58 (1998) 7260.
[14] G. Zheng, M. Lundberg, J. Jakowski, et al., Int. J. Quantum Chem. 109 (2007) 1841.
[15] W.A. Goddard III, A.C.T. van Duin, K. Chenoweth, et al., Topics in Catal. 38 (2006) 93.
[16] W.J. Mortier, S.K. Ghosh, S. Shankar, J. Am. Chem. Soc 108 (1986) 4315.
[17] Y. Cong, Z.-Z. Yang, Chem. Phys. Lett. 316 (2000) 324.
[18] P.S. Krstic, J.P. Allain, A. Allouche, et al., Fusion Eng. Design 87 (2012) 1732.
[19] P.S. Krstic, J.P. Allain, C.N. Taylor, et al., Phys. Rev. Lett. 110 (2013) 105001.
[20] C.N. Taylor, J. Dadras, K.E. Luitjohan, J.P. Allain, P.S. Krstic, C.H. Skinner, J. Appl. Phys. 114 (2013) 223301.
[21] S.S. Harilal, J.P. Allain, A. Hassanein, M.R. Hendricks, M. Nieto-Perez, Appl. Surface Sci. 255 (2009) 8539.
[22] J.P. Allain, C.N. Taylor, Phys. Plasmas 19 (2012) 056126.